

# Microwave Electronics as an enabling information technology

Alessandro Cidronali

Dept. Information Engineering, University of Florence, Italy





# Posizione Attuale

- Dal 23.12. 2011 svolgo l'attività di **Professore Associato di Elettronica (ING\INF-01)** presso il DINFO, conferma in ruolo con decorrenza 23.12.2014;
  - Ambito di ricerca: **elettronica delle microonde e onde millimetriche;**
  - Didattica:
    - **Elettronica dei Sistemi a Radiofrequenza** CdS - Ingegneria Elettronica e TLC
    - **Dispositivo per la Micro e Nano Elettronica** CLM – Elettronica
  - Membro del collegio dei docenti del Dottorato di Ricerca *Pegaso ‘Smart Industry’*
- Ho ottenuto **l'Abilitazione Scientifica Nazionale di I Fascia**, per il settore concorsuale **09/E3 – ELETTRONICA il 20 Luglio 2017**



# Posizione Attuale

- Membro eletto della **Commissione di Indirizzo e Autovalutazione** del DINFO;
- Dal 13 Giugno 2017 ho assunto il ruolo di **Direttore del Centro Interdipartimentale per le Tecnologie e Microsistemi per la Sicurezza e Qualità Ambientale** dell'Università di Firenze;
- Dal 7 Giugno 2019 assume il ruolo di **Responsabile scientifico del Laboratorio Congiunto in “Tecnologie e Sistemi per l’Info-Mobilità”** tra la **Società Autostrade Tech e DINFO**;
- Membro del comitato di gestione del Centro di Ricerche interuniversitario **Microwave Engineering for Space Applications (MECSA)**



**DINFO**

Dipartimento di  
Ingegneria dell'Informazione

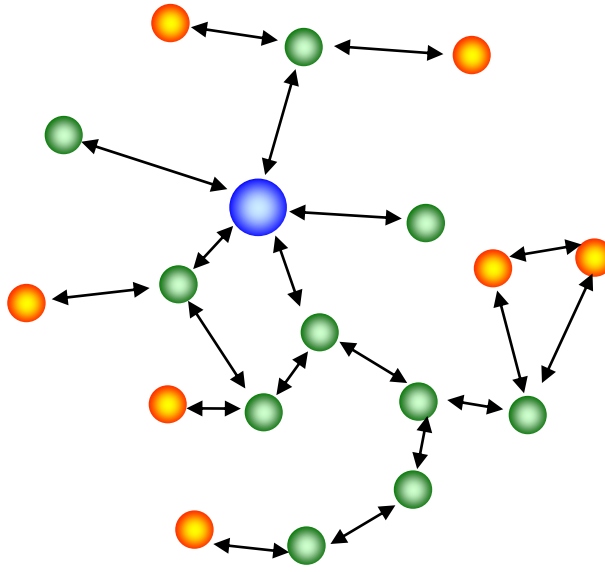
# Il Centro Interdip. per le Tecnologie e Microsistemi per la Sicurezza e Qualità Ambientale:

- Consocia **4 Dipartimenti UniFI** e **18 docenti/ricercatori/tecnic**i
- Si occupa prevalentemente di attività di ricerca e disseminazione nell’ambito del **monitoraggio ambientale** per finalità di controllo e sicurezza

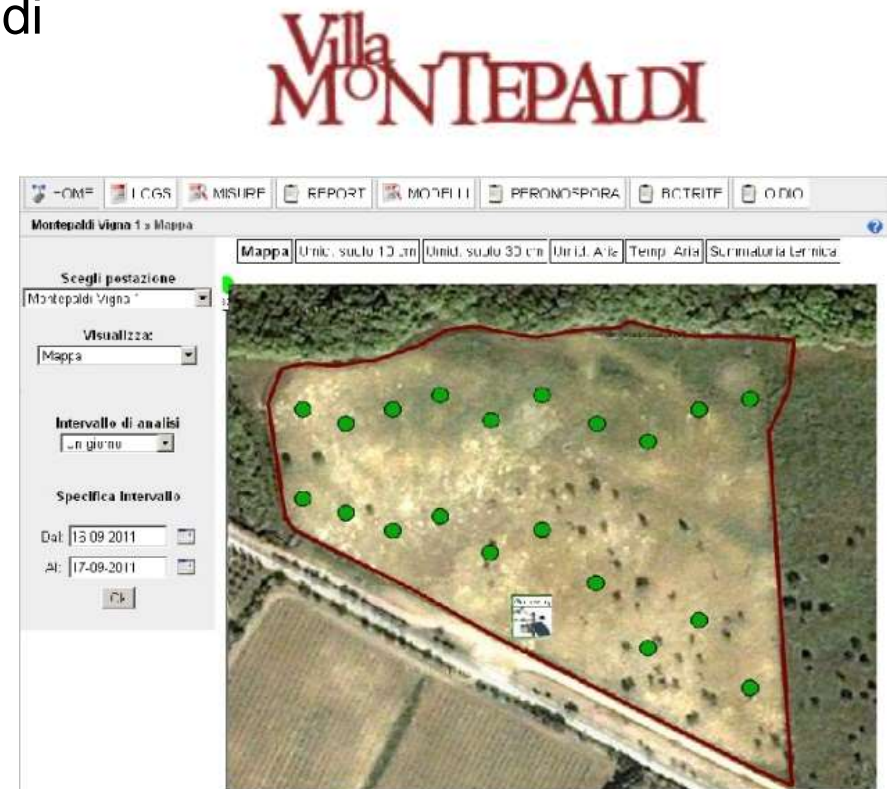


## Distributed Integrated System for Vineyard

Impiego di wireless sensors network per il monitoraggio della vigna  
dell'azienda universitaria di Montepaldi

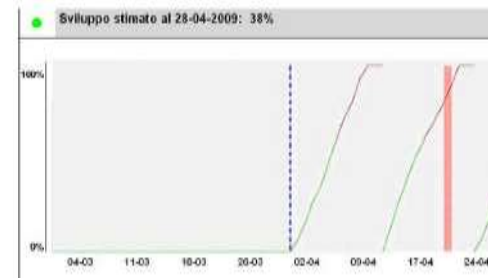
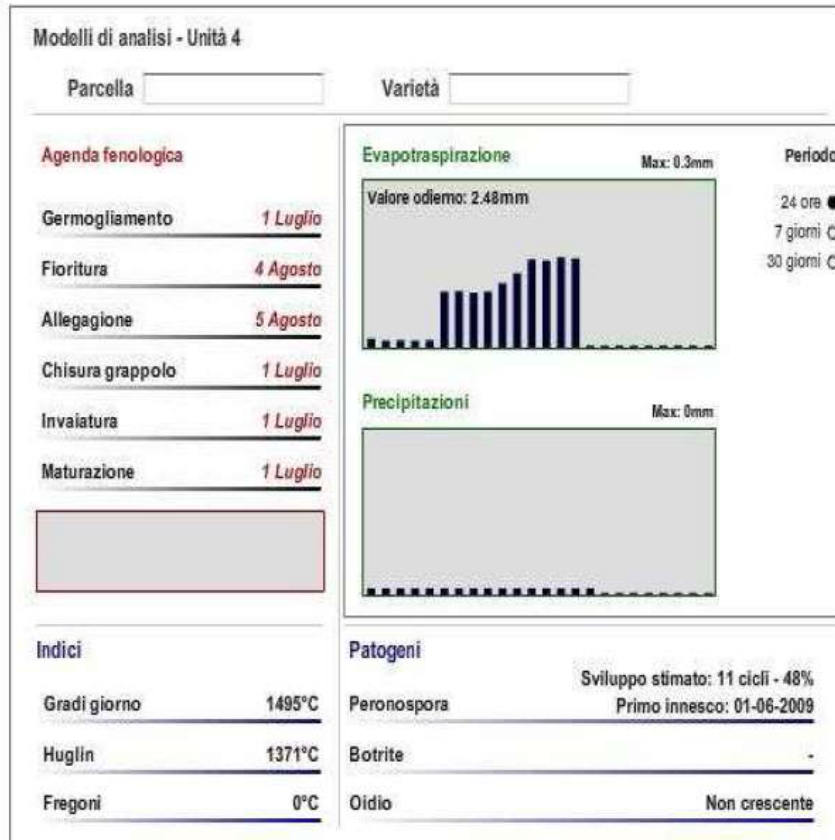


- PAN coordinator
- Full Function Device
- Reduced Function Device

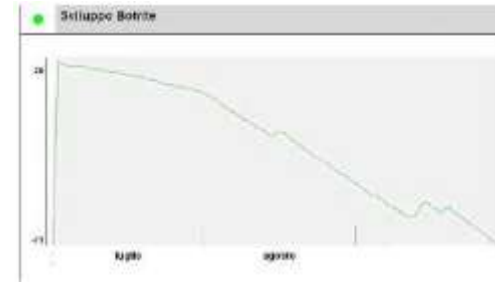


## Distributed Integrated System for Vineyard

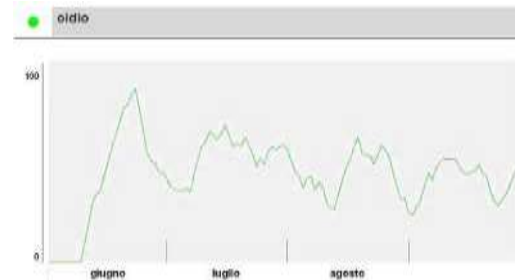
# Previsione degli attacchi di patogeni per la somministrazione adattiva di trattamenti



Previsione attacco  
Peronospera



Previsione attacco  
Botrite



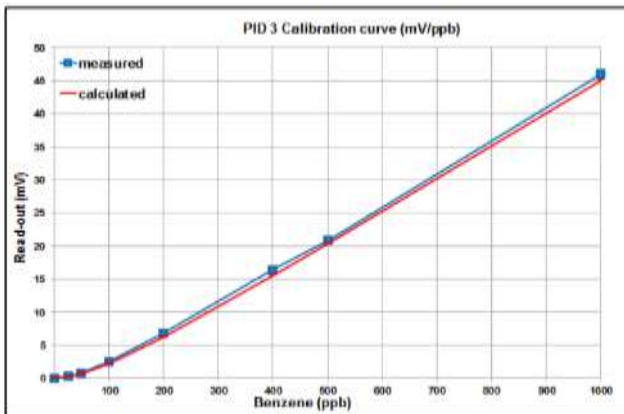
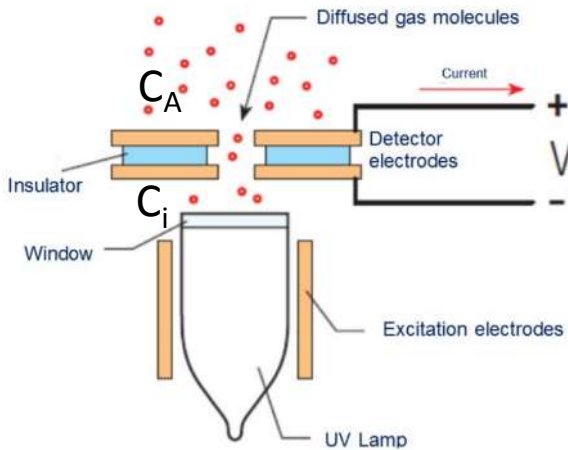
Previsione  
attacco Oidio

Distributed Integrated System for Volatile Organic Compound (VOC) Monitoring": rete presso lo stabilimento petrolchimico di Mantova



Photoionization detectors (PIPs) measure VOCs and other toxic gases in low concentrations from ppb up to 10,000 ppm.

Gas molecule ionization yields a current determined by opposite-polarity ions collected by a pair of electrodes.



- The PID operation principle is governed by the Fick's first law, which provide the analyte,  $J$ , diffusion

$$J = \frac{1}{A_C} \frac{\partial n(t)}{\partial t} = -D \frac{\partial C}{\partial x}$$

- Introducing the diffusivity length,  $L_d$ , and ionization time  $\tau_i$ :

$$J_D = \frac{1}{A_C} \left. \frac{\partial n}{\partial t} \right|_{x=0} = D \frac{(C_A - C_{io})}{L_d} , \quad \frac{\partial C_i(t)}{\partial t} = K I_n \frac{\sigma}{S} C_i = K \frac{C_i}{\tau_i} = \frac{C_i}{\tau_i}$$

- The calibration process involves the readout measurements at various  $C_i$  (ppb)

$$\alpha_n = (C_i)_n = \frac{V_n}{S_{v,n}} = \frac{V_{OUT,n}}{S_{v,n} \cdot G}$$

- then the classical PID zero/span calibration curve should be modified to represent the nonlinear behavior in the **low-ppb range**

$$V(C_A) = \alpha S_v C_A = \frac{C_A^2}{C_A + C_o} S_v$$



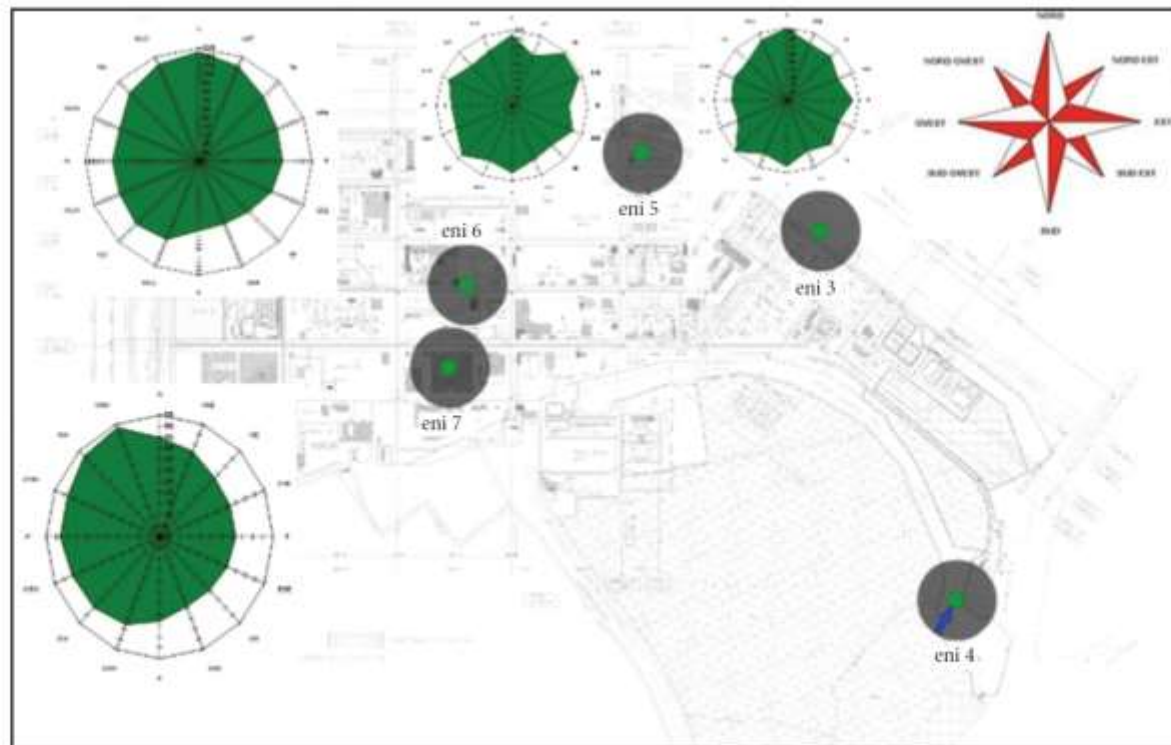
**DINFO**

Dipartimento di  
Ingegneria dell'Informazione

monitoraggio qualità  
dell'ambiente

“Distributed Integrated System for Volatile Organic Compound (VOC) Monitoring”: rete  
presso lo stabilimento petrolchimico di Mantova

Fusione dati VOC – dati ambientali (direzione e intensità del vento)

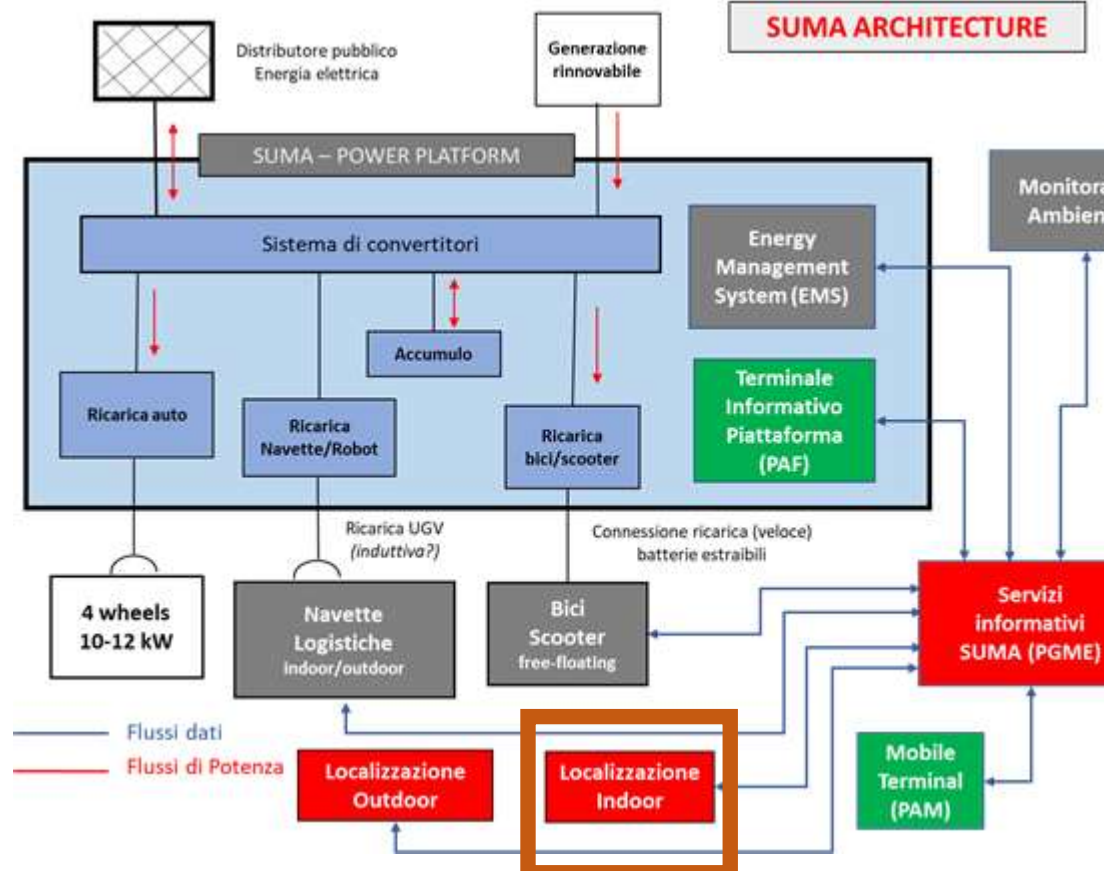


**DINFO**Dipartimento di  
Ingegneria dell'Informazione

# Struttura Urbana Multifunzionale Attiva (SUMA)



Regione Toscana

Scuola Superiore  
Sant'AnnaUNIVERSITÀ  
DEGLI STUDI  
FIRENZE

Radiazione solare Visible-UV,  
Qualità dell'aria: NO<sub>2</sub>, NO, O<sub>3</sub>,  
H<sub>2</sub>S, SO<sub>2</sub>, CO, VOC (Volatile  
Organic Compound)  
PM10, PM2,5

# Indoor wireless localization technology

- Assuming a multi-bean radio device, (the anchor), an anchors constellation reads an array of Received Signal Strength Indicator (**RSSI**),  $\text{dim}(\text{RSSI})=N \times M$
- the simplest analytical search Localization reduces to the solution of the following Least Square Estimator

The observation model is

$$\text{RSSI}_n = G_n(\hat{\theta}) + P_{inc} + w$$

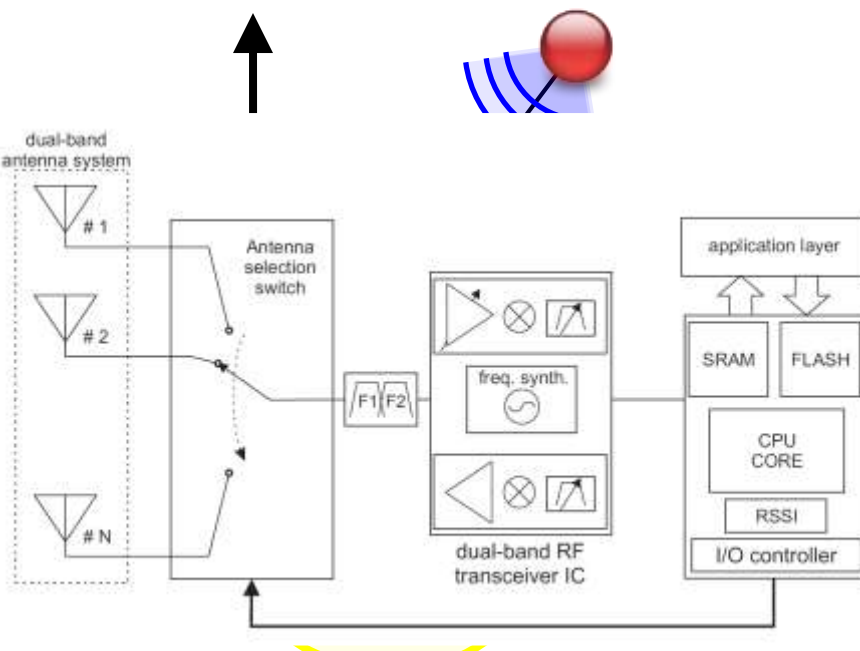
s compared with the incident power from the ic source in position  $(x, y)$ , at distance  $D$  from the anchor

$$P_{inc}(D) = P_{tx}(x, y) + 20 \log (4\pi D/\lambda_0)$$

We assume the cost function the variance of difference between the steering vector and the received signal map

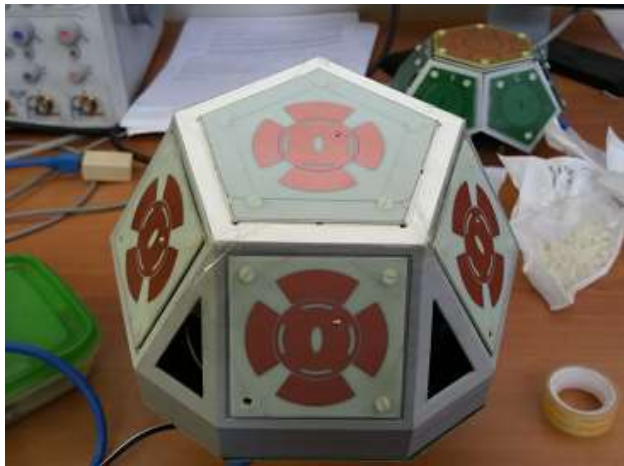
$$C(x, y) = \frac{1}{MN} \sum_{i=1}^{MN} \left[ (s_i - m_i) - \frac{1}{MN} \sum_{j=1}^{MN} (s_j - m_j) \right]^2$$

$$(\hat{x}, \hat{y}) = \operatorname{argmin} \{ C(x, y) \}$$



# Indoor wireless localization technology

- By the Fisher Information Matrix ( $\mathcal{F}$ ) the accuracy of a DoA estimation is achieved *a-priori*
  - For the 2D case in exam the FIM is defined as

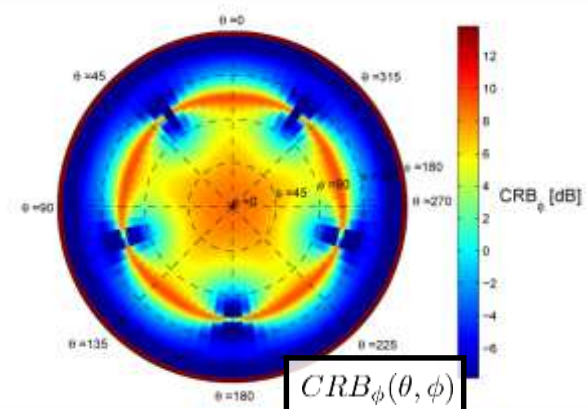
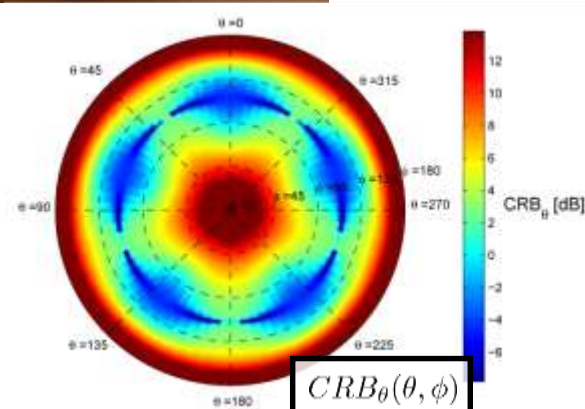


$$\text{CRB}_x(x, y) = [\mathcal{F}]^{-1}|_{2,2} = \sigma_{RSSI}^2 \frac{\sum_{n=1}^{NM} \left[ \frac{\partial G_n}{\partial x} \right]^2}{\text{Det}[\mathcal{F}]}$$

$$\text{CRB}_y(x, y) = [\mathcal{F}]^{-1}|_{1,1} = \sigma_{RSSI}^2 \frac{\sum_{n=1}^{NM} \left[ \frac{\partial G_n}{\partial y} \right]^2}{\text{Det}[\mathcal{F}]}$$

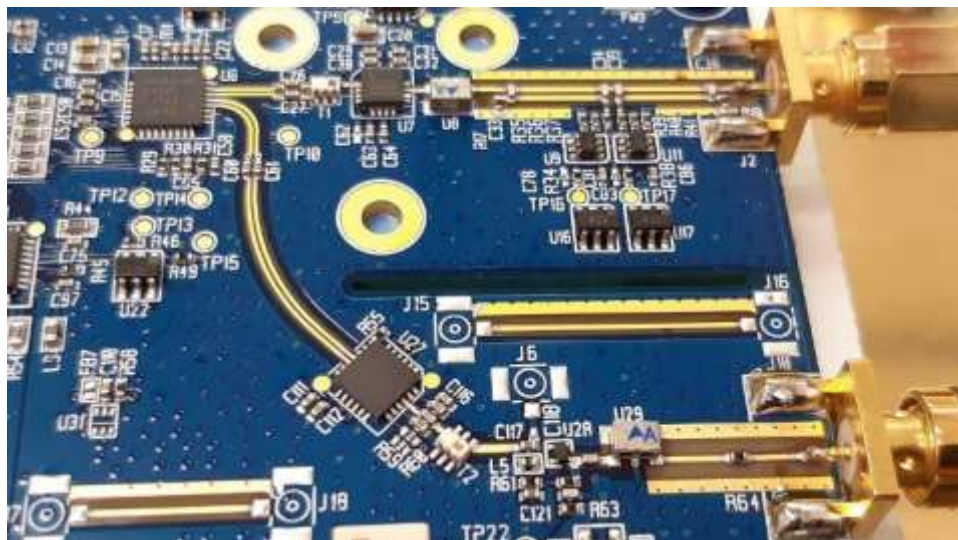
therefore, for any unbiased position estimator:

$$\text{Var}[E] \geq \text{CRB}(x, y) = \text{CRB}_x(x, y) + \text{CRB}_y(x, y)$$

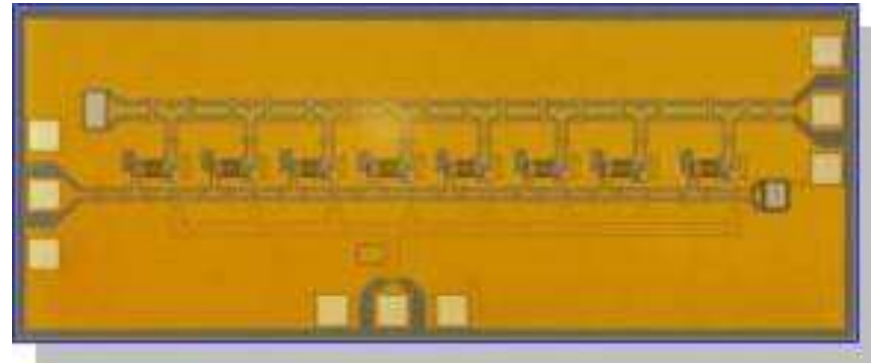


## A brief introduction

Example of systems and circuits investigated and developed



high dynamic range full-duplex DSRC transceivers



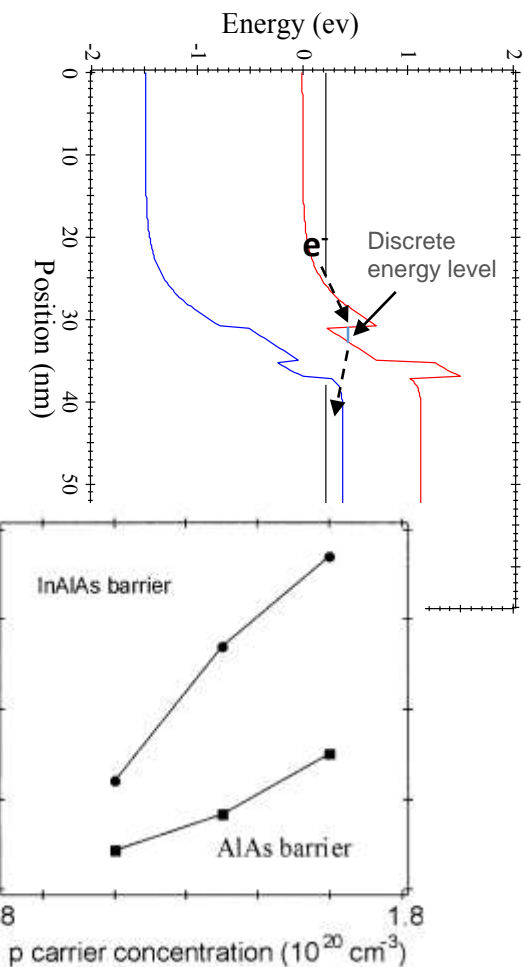
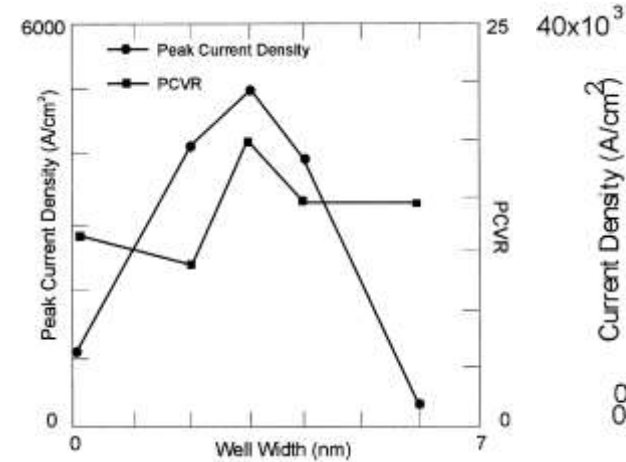
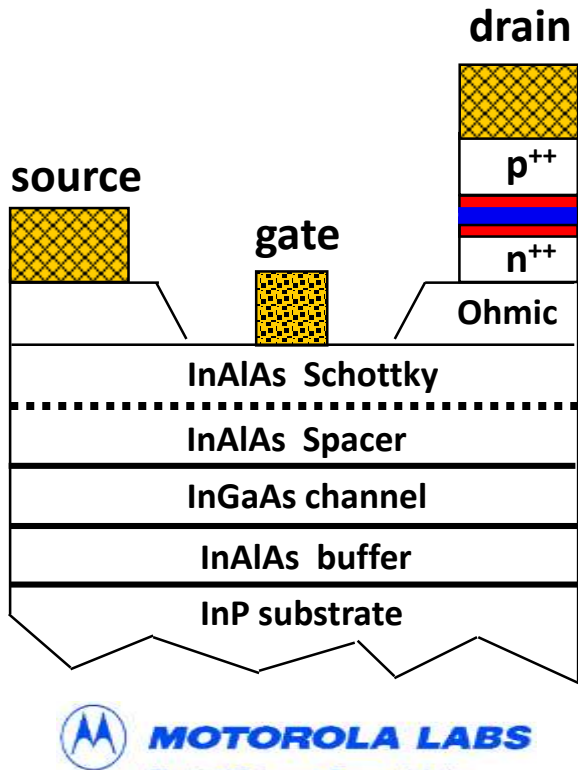
0.1 – 40 GHz bandwidth Travelling Wave Amplifier in 0.2um GaAs HEMT technology



Doherty Power Amplifier DVBT 300 W peak power  
in Si-LDMOS technology

## A brief introduction

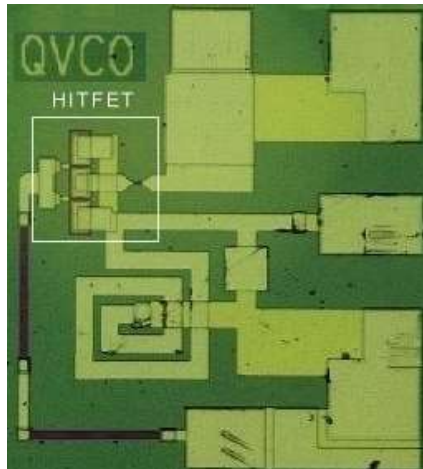
Device modeling investigation: quantum functional device based on *interband resonant tunneling*



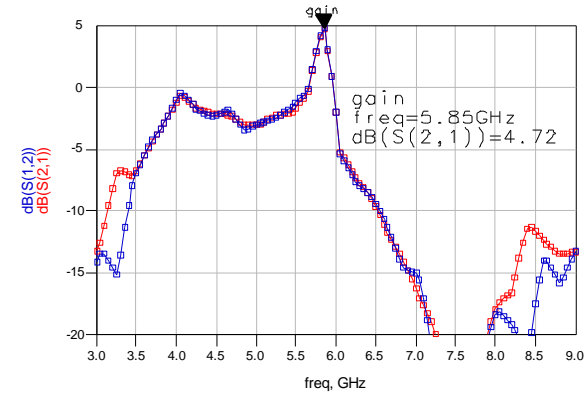
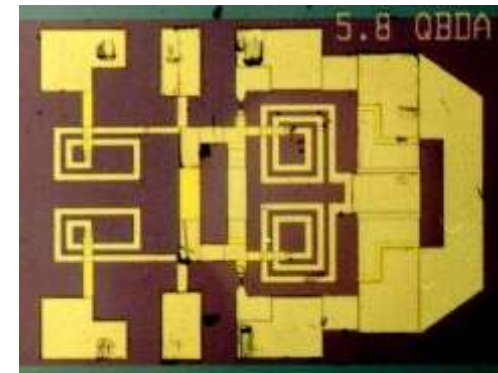
**DINFO**Dipartimento di  
Ingegneria dell'Informazione

# Research activity on microwave electronics

The research was motivated by the potential development of building blocks in Microwave Monolithic Integrated Circuit (Quantum MMIC) technology operating at extremely low supply voltage and reduced number of devices



output frequency	6.18 GHz
output power	-16dBm
tuning range	140 MHz
SSCR	-105dBc/Hz @ 5MHz
efficiency	3%
power supply	850µW
supply voltage	500mV
die size	450x550µm <sup>2</sup>

**MOTOROLA LABS**  
Physical Sciences Research Labs

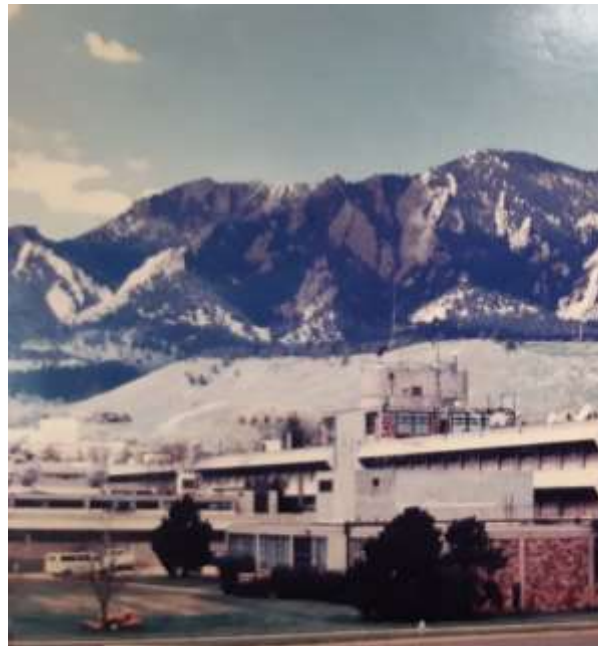


**DINFO**

Dipartimento di  
Ingegneria dell'Informazione

# Nonlinear Dynamic Microwave Systems Characterization

at the “RF nonlinear characterization group” of the National Institute for  
Standard and Technology, Boulder (CO) USA



Prof K. C. Gupta, Ale, Dr. J. Jargon, and Dr K. Ramley



## A brief introduction

A general nonlinear system with memory is described by the multidimensional convolution integral, i.e. the Volterra Series

$$i(t) = \sum_{n=1}^N a_n \int_{-\infty}^{+\infty} \cdots \int_{-\infty}^{+\infty} h_n(\tau_1, \dots, \tau_n) v(t - \tau_1) \dots v(t - \tau_n) d\tau_n \dots d\tau_1$$

with  $N=1$  it describes a linear dynamic system.

*In the case of system memory duration  $\tau_\infty$  small compared to the inverse of excitation signal bandwidth  $B_W \rightarrow B_W x \tau_\infty \ll 1$ , the series converges to the **Modified Volterra Series***

$$i(t) = F_{DC}(v(t)) + \int_0^{\tau_m} h(v(\tau), \tau) [v(t - \tau) - v(t)] d\tau$$



# Nonlinear Dynamic Microwave Systems Characterization

## A brief introduction

Under the assumption of the small-memory the term  $[v(t - \tau) - v(t)]$  becomes a linearization of the large-signal,  $v_{LS}(t)$ , applied to the system

$$i(t) = F_{DC}(v(t)) + \sum_1^N f^{(n)} \cdot \frac{d^n v}{dt^n}$$

with

$$f^{(n)}(v(t)) = \frac{1}{n!} \int_0^{\tau_m} h(v, \tau) \cdot \tau^n d\tau$$

coefficients to be determined.

The model can be conveniently identified in frequency domain

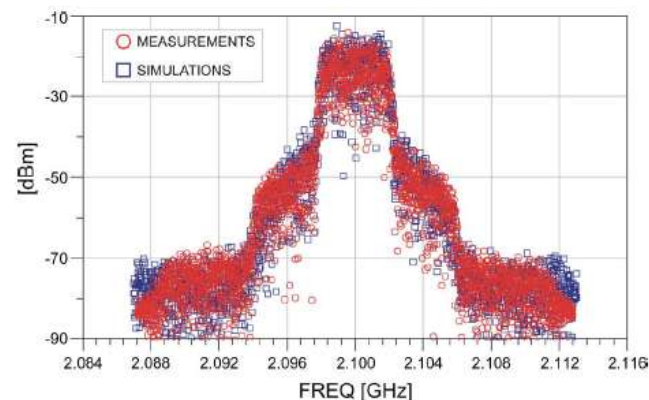
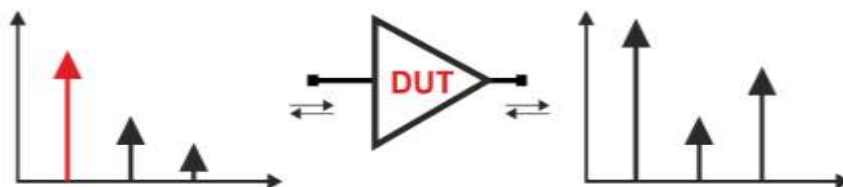


Fig. 20. Comparison between simulated and modeled single carrier WCDMA at 2.1 GHz.

# Nonlinear Dynamic Microwave Systems Characterization

Transforming into the frequency domain and introducing the concept of waves,



$$b_{1,k} = F_{1,k} (a_{1,1}, a_{1,2}, \dots, a_{2,1}, a_{2,2}, \dots)$$

$$b_{2,k} = F_{2,k} (a_{1,1}, a_{1,2}, \dots, a_{2,1}, a_{2,2}, \dots)$$

the linearization about the Large-Signal Operating Point (LSOP), lead to

- $i$ : number of system port;  $k$ : index of the harmonic
- If only one incident pseudo-wave,  $a_{1,1}$ , is large then the other smaller inputs can be linearized about the large-signal response of  $F_{i,k}$  to only  $a_{1,1}$ . includes exact nonlinear mapping

$$b_{i,k} = F_{i,k} (|a_{1,1}|, a_{1,2}P^{-2}, a_{1,3}P^{-3}, \dots) P^k \approx F_{i,k} (|a_{1,1}|, 0, 0, \dots) P^k$$

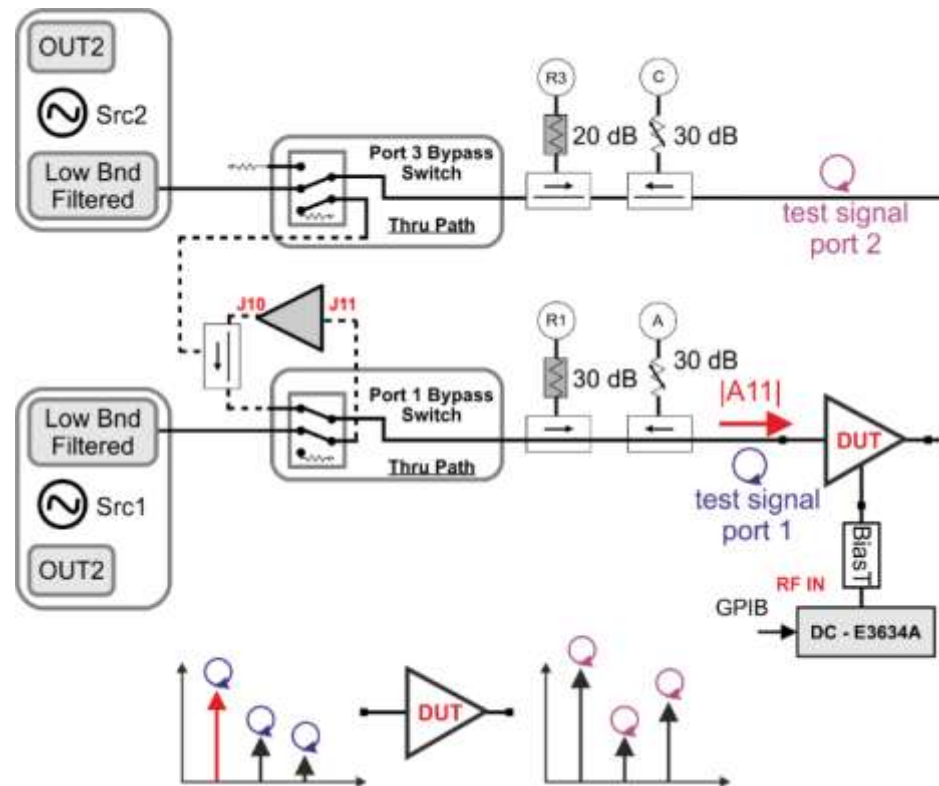
$$+ \sum_{k,l \neq (1,1)} \left[ \frac{\partial F_{i,k}}{\partial (a_{kl}P^{-l})} \Big|_{|a_{11}|} \cdot a_{kl}P^{k-l} + \frac{\partial F_{i,k}}{\partial (a_{kl}P^{-l})^*} \Big|_{|a_{11}|} \cdot a_{kl}^*P^{k+l} \right]$$

to totally linear non-analytic map

$$P = \frac{a_{1,1}}{|a_{1,1}|} = e^{j * \arg(a_{1,1})}$$

# Nonlinear Dynamic Microwave Systems Characterization

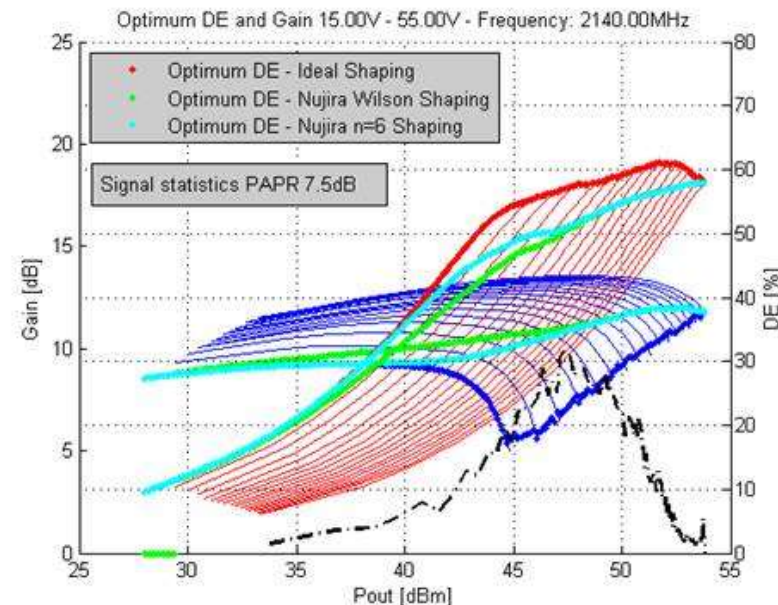
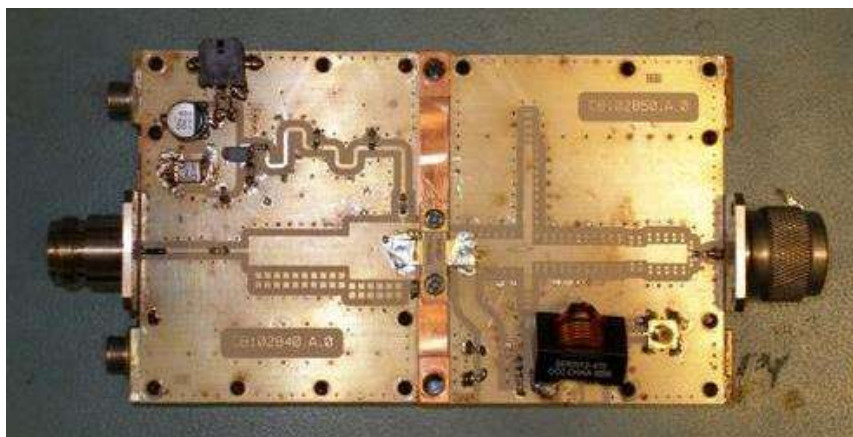
- The setup is based on a calibrated multi-port transmitters - coherent receivers
- The absolute value of harmonics amplitude and phase is measured
- The technique: injects a drive large-signal at the device input and sequentially a test signal at each port and to all fundamentals and harmonics.
- The test signal phase is rotated at steps around 360 degrees



# Development of a Envelope Tracking Power

Dual-band GaN based ET-PA, developed by **probability conscious approach**

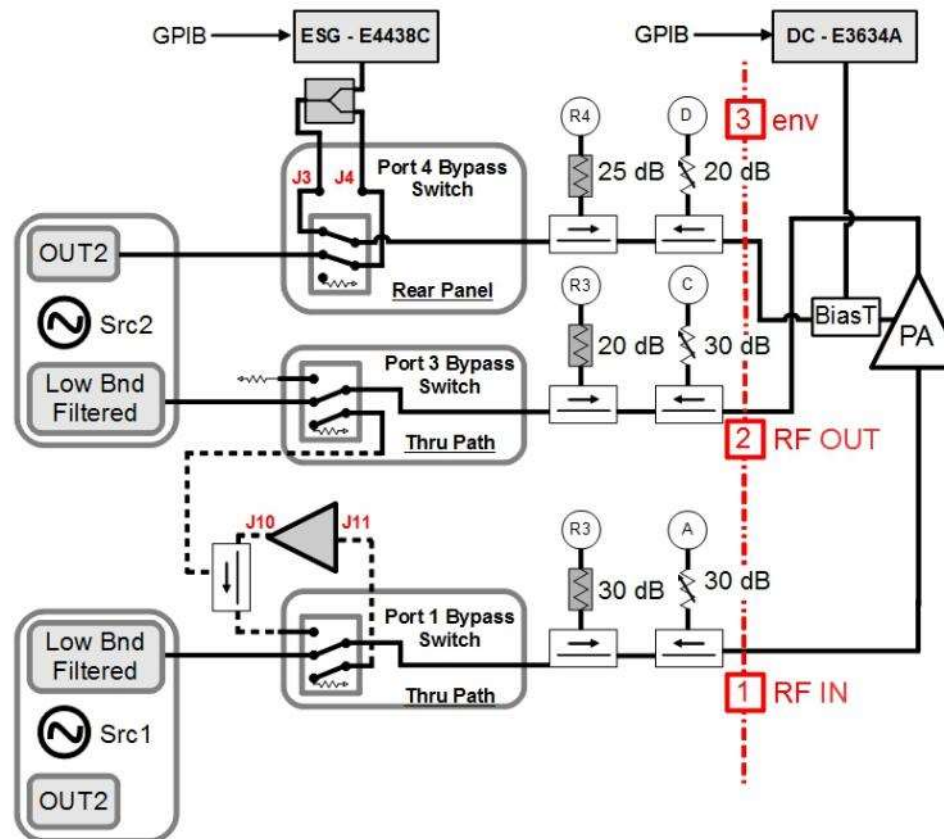
- The signal distribution imposes the estimation of the optimum impedance on mean value basis
- Shaping table, that is the law  $V_{dc}$  vs  $P_{in}$ , is critical in the ET-PA



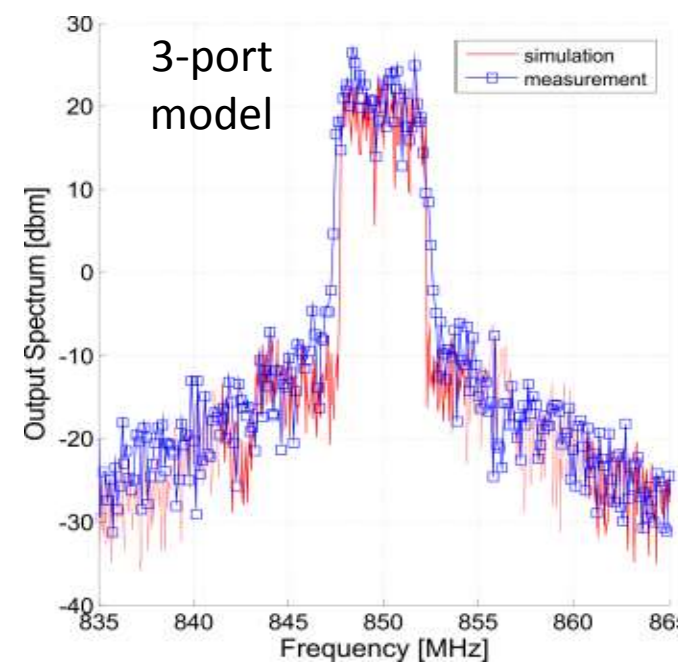
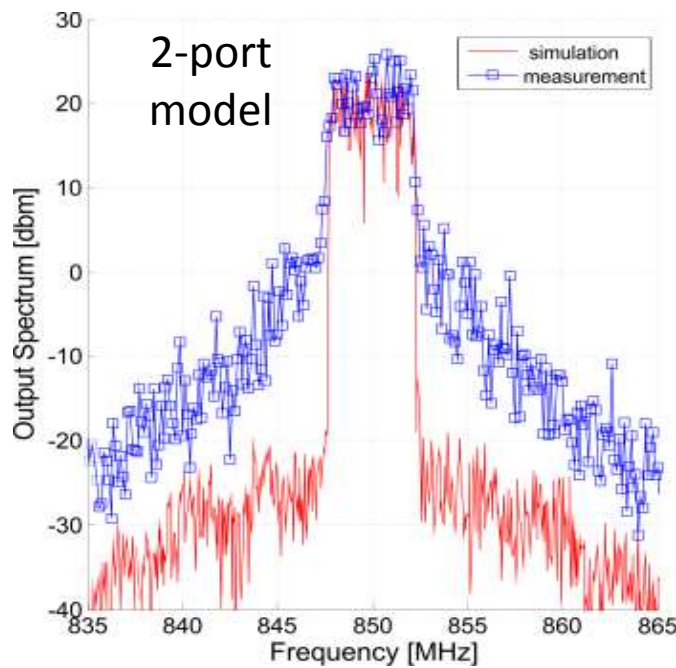
# Nonlinear Vector Characterization: Envelope Tracking PA modeling

3-port ET-PA dynamic model of

- Extracted by a 3-channel Nonlinear VNA based set up



# Nonlinear Vector Characterization: Envelope Tracking PA modeling

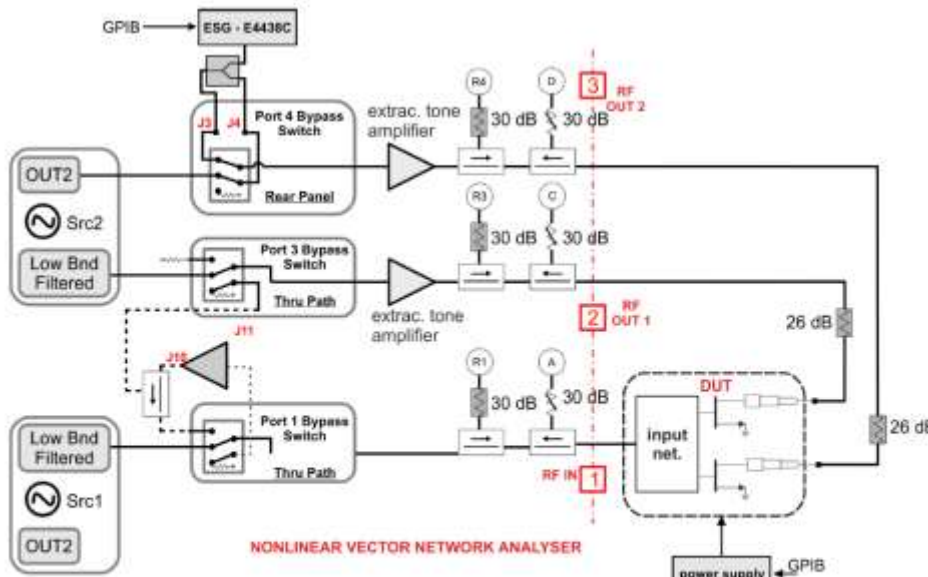


Comparison between measured and simulated LTE5 spectra at the ET system output for at 35.5 dBm output power.

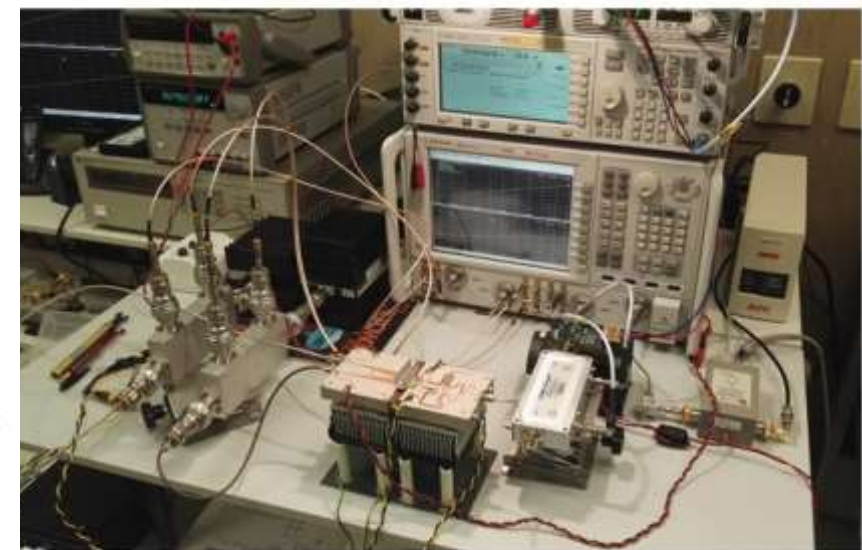
model	Measured [dB]		Simulated [dB]	
	ACLRlow	ACLRup	ACLRlow	ACLRup
2-port	-27.1	-25.3	-44.2	-44.2
3-port	-32.0	-29.1	-31.1	-31.1

# Nonlinear Vector Characterization: the Doherty PA optimization

## Si-LDMOS UHF Doherty High-Power Amplifier Design by 3-port subcircuit characterization



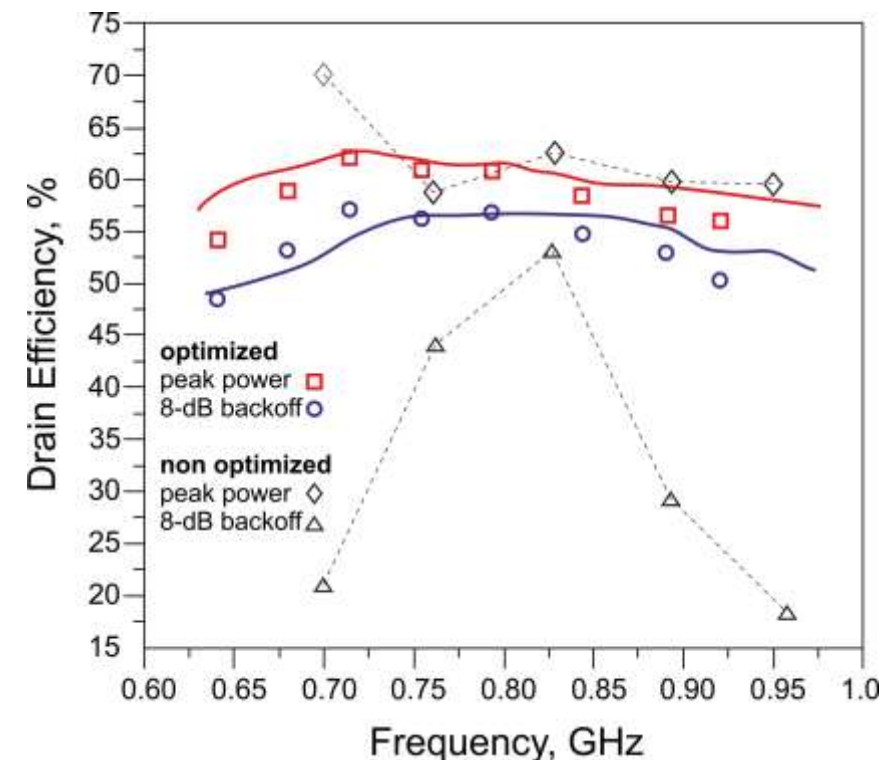
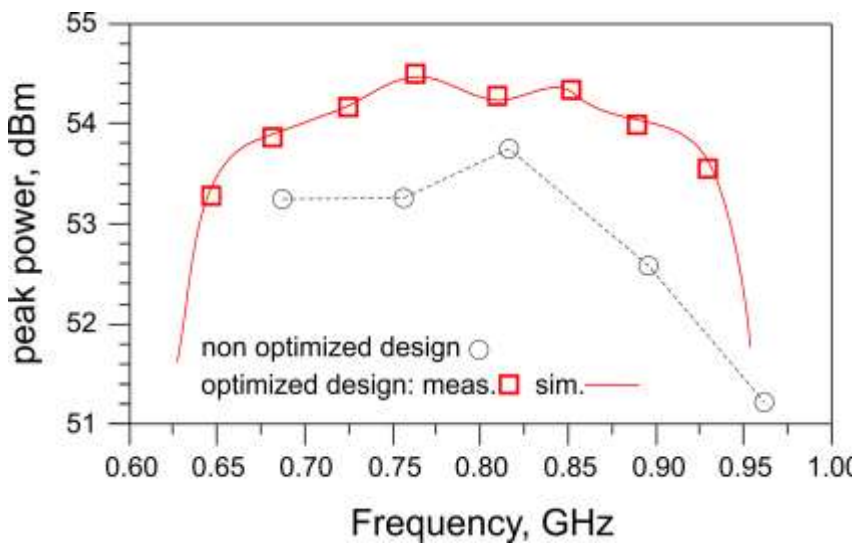
(a) Schematic of the 3-port NVNA based setup for the RF devices pair characterization.



(b) Picture of the 3-port NVNA set-up

# Nonlinear Vector Characterization: the Doherty PA optimization

## Si-LDMOS UHF Doherty High-Power Amplifier Design by 3-port subcircuit characterization



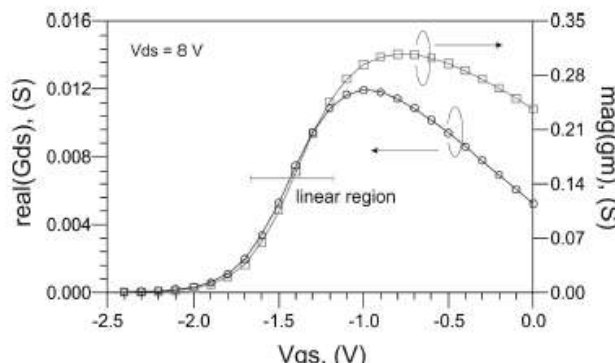
# Subsystems for GaN-based Radar

- Gallium Nitride (GaN) is an emerging s.c. technology for high power, high frequency applications
- We investigated its properties for highly linear Ka-band GaN-on-Si **MMIC Down-Conversion Active Balanced Mixer** for Radar Applications
- The conversion properties of a GaN-HEMT contains the LO

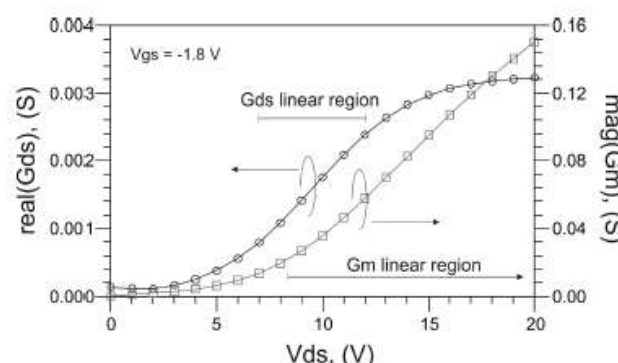
$$I_{ds} = I_{ds}^{DC} + g_m v_{gs} + g_{ds} v_{ds} + \frac{1}{2} \frac{\partial g_m}{\partial v_{gs}} v_{gs}^2 + \frac{1}{2} \frac{\partial g_{ds}}{\partial v_{ds}} v_{ds}^2$$

$$+ \frac{\partial g_m}{\partial v_{ds}} v_{gs} v_{ds} + \frac{1}{6} \frac{\partial^2 g_m}{\partial^2 v_{gs}} v_{gs}^3 + \frac{1}{2} \frac{\partial^2 g_{ds}}{\partial^2 v_{gs}} v_{gs}^2 v_{ds} + \frac{1}{2} \frac{\partial^2 g_m}{\partial^2 v_{ds}} v_{gs} v_{ds}^2 + \frac{1}{6} \frac{\partial^2 g_{ds}}{\partial^2 v_{ds}} v_{ds}^3$$

conversion                          2<sup>nd</sup> order intermodulation                          Taylor expansion, where the term  $v_{gs}$   
V<sub>ds</sub> is set to 0 by a resonant short circuit



(a) Function of static drain voltage



(b) Function of static source voltage

Fig. 1. Simulation of the quasi-static  $g_m$  and  $g_{ds}$  device behavior.

# Subsystems for GaN-based Radar

- Gallium Nitride is an emerging semiconductor technology for high power, high frequency applications
- We have investigated its properties for highly linear Ka-band GaN-on-Si MMIC Down-Conversion Active Balanced Mixer for Radar Applications
- The conversion properties of a GaN-HEMT are described by the Taylor expansion, where the term  $v_{gs}$  contains the LO

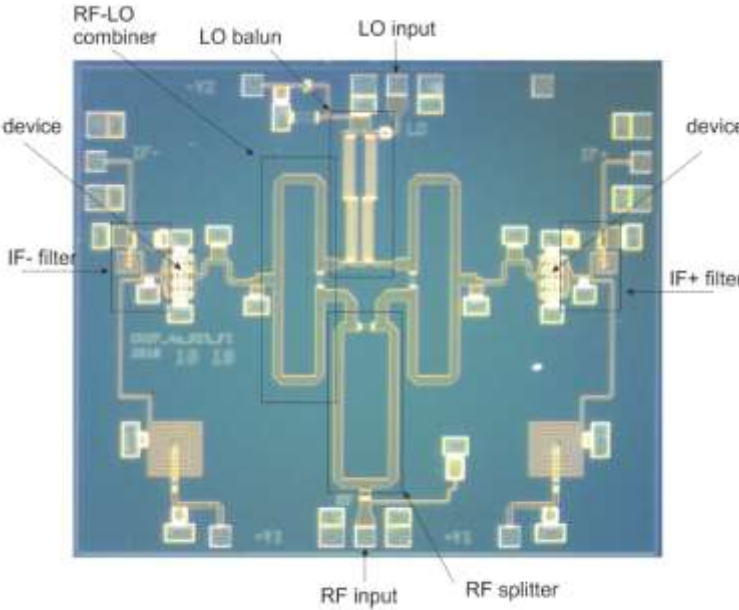


Fig. 3. The balanced mixer prototype chip photograph

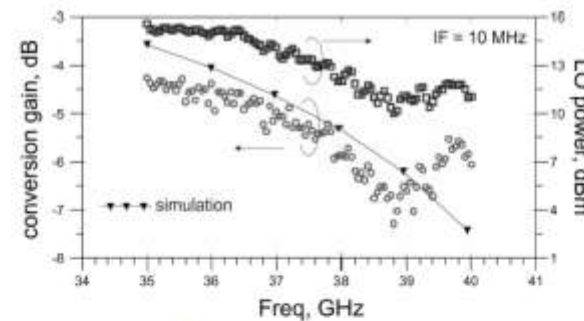
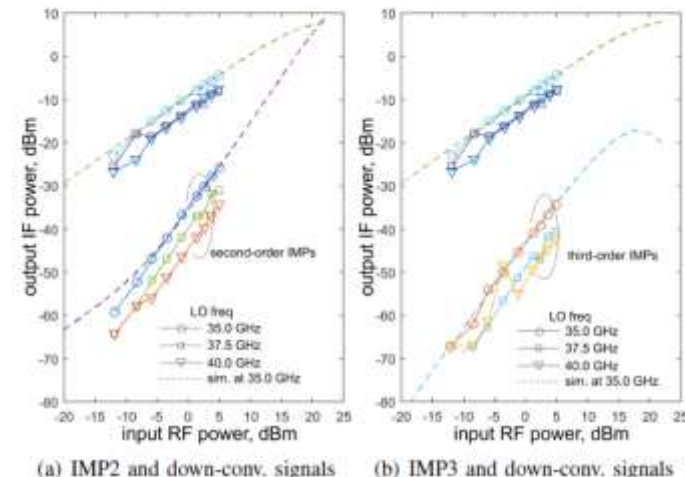


Fig. 4. Measured CG with calibrated 4-port VNA in mixer vector mode.





**DINFO**

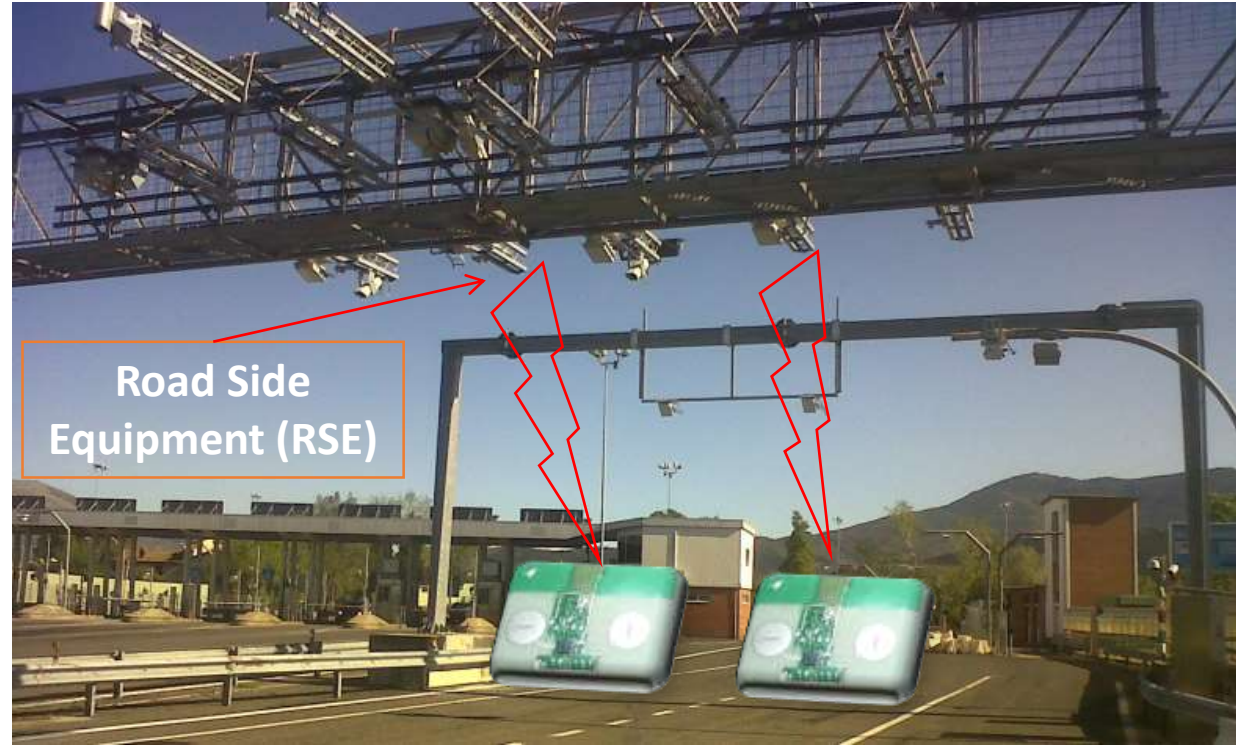
Dipartimento di  
Ingegneria dell'Informazione

# Dedicated Short Range Vehicular Communications technologies

Sistema multi-lane free-flow per il pedaggio autostradale



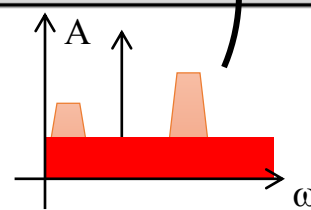
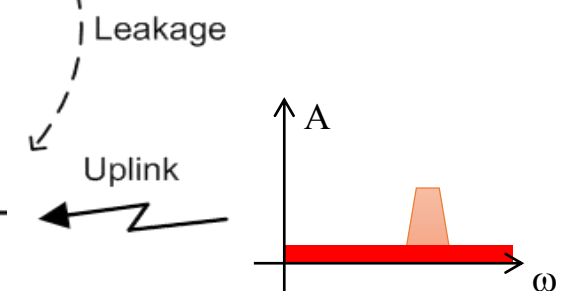
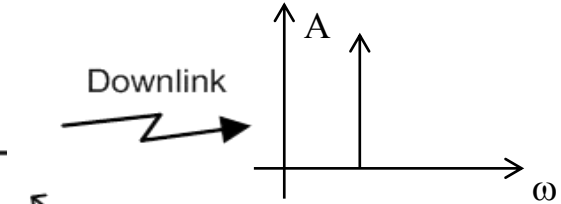
On-board unit)



Attività svolta nell'ambito del **Laboratorio Congiunto “Tecnologie e Sistemi per l’Info-Mobilità”** tra **DINFO** e la **Società Autostrade-Tech** **autostrade//Tech**

# Dedicated Short Range Vehicular Communications technologies

- The self-interference determines
  - an increase of LNA noise figure
  - higher levels of the required down converter SFDR

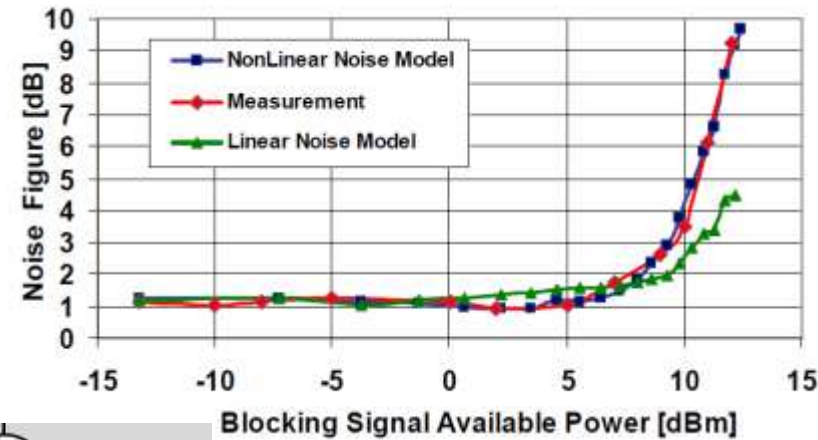
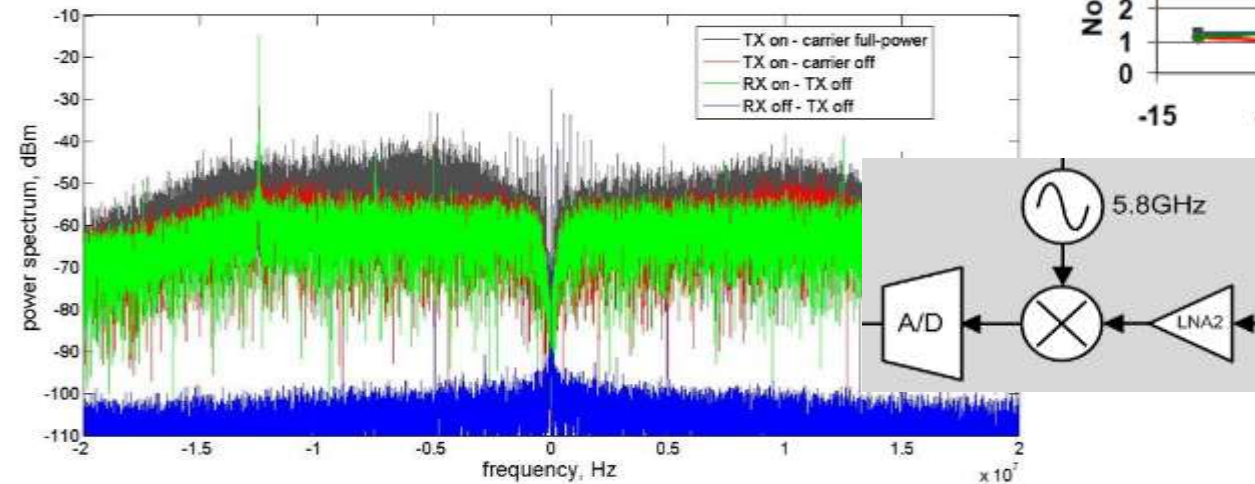


# Dedicated Short Range Vehicular Communications technologies

## NF increases with the interference strength

- Example of GaAs PHEMT LNA driven beyond P-1dB
  - Linear model: bias dependent noise source modulation
  - Nonlinear model: noise source correlation and conversion

DSRC spectrum at the Rx baseband: subcarrier at 1.5 MHz  
signal 16 ks digitized by a 16 bit ADC at 40 Msps



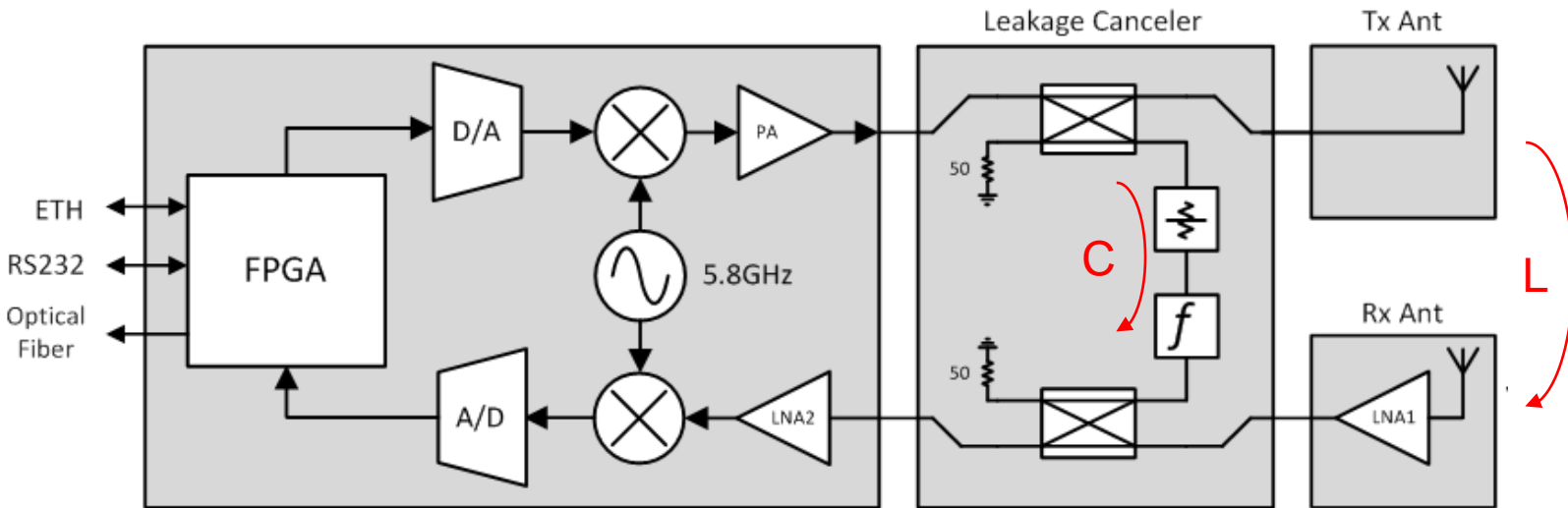
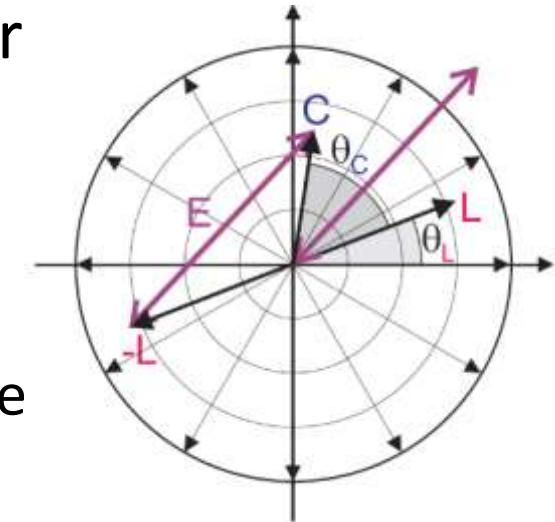
$$F = \frac{N_0^{(Nlin)}}{K_B T G_T^{(Nlin)}}$$

# Dedicated Short Range Vehicular Communications technologies

- Canceler operation principle: from the Car theorem

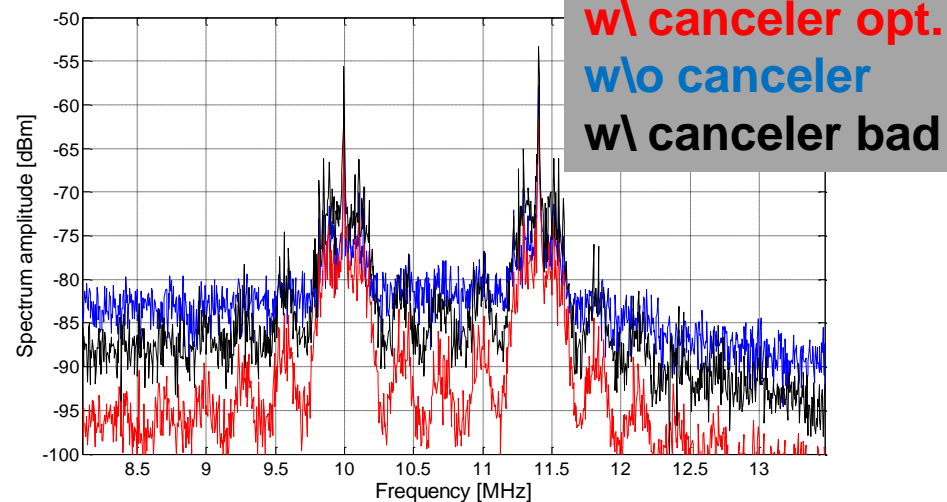
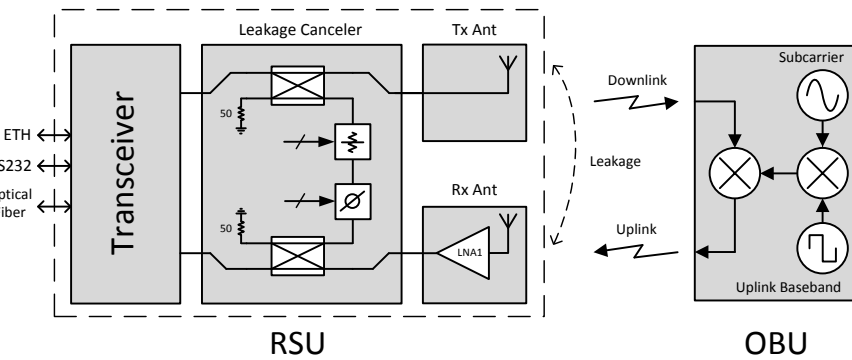
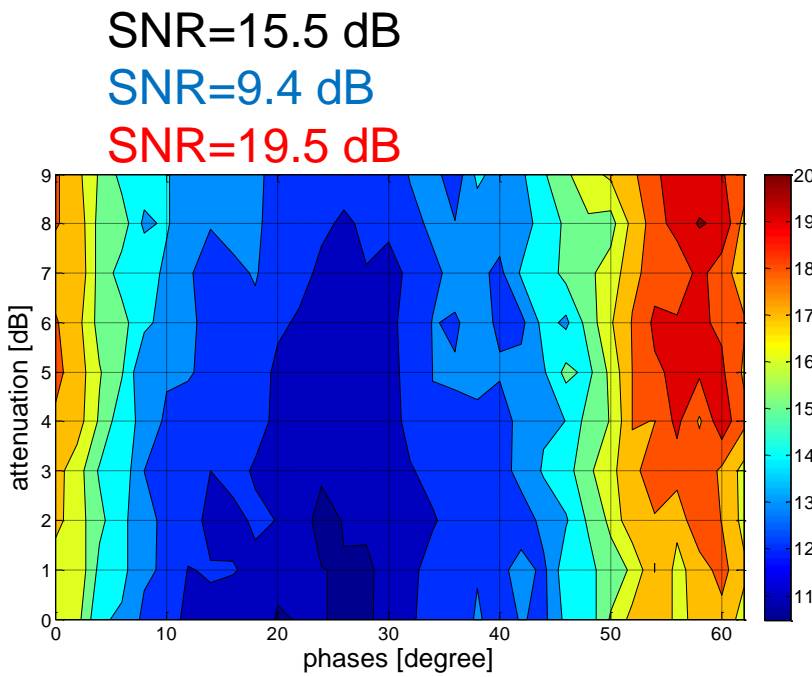
$$E = \sqrt{|L|^2 + |C|^2 + 2|L||C| \cos(\theta_C - \theta_L)}$$

- For  $L/C=1$  and  $\theta_C - \theta_L = \pi$  the cancellation of the perfect



# Dedicated Short Range Vehicular Communications technologies

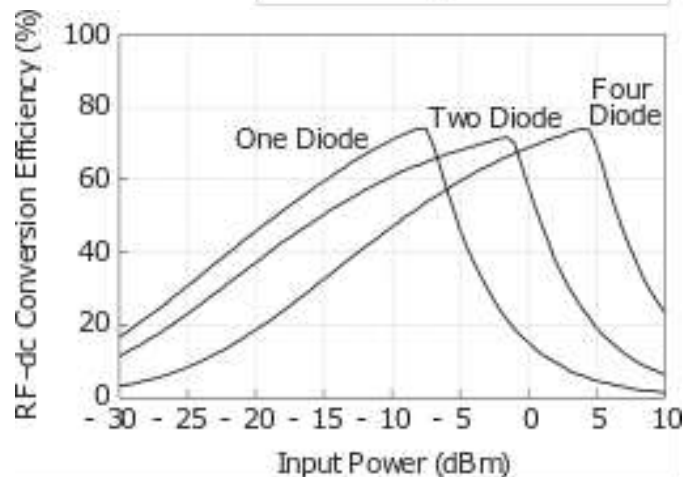
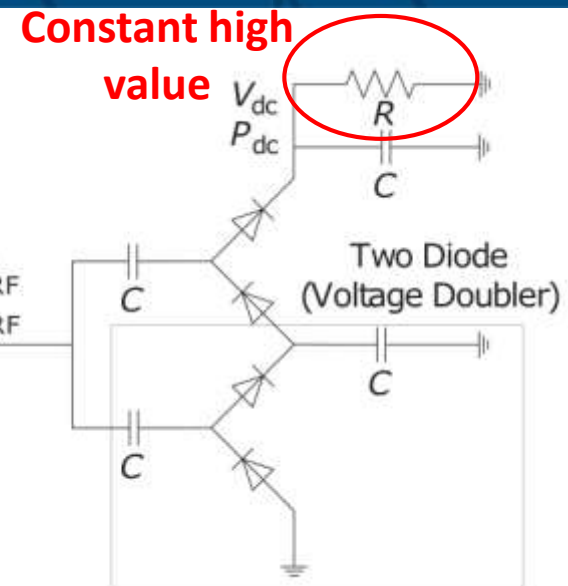
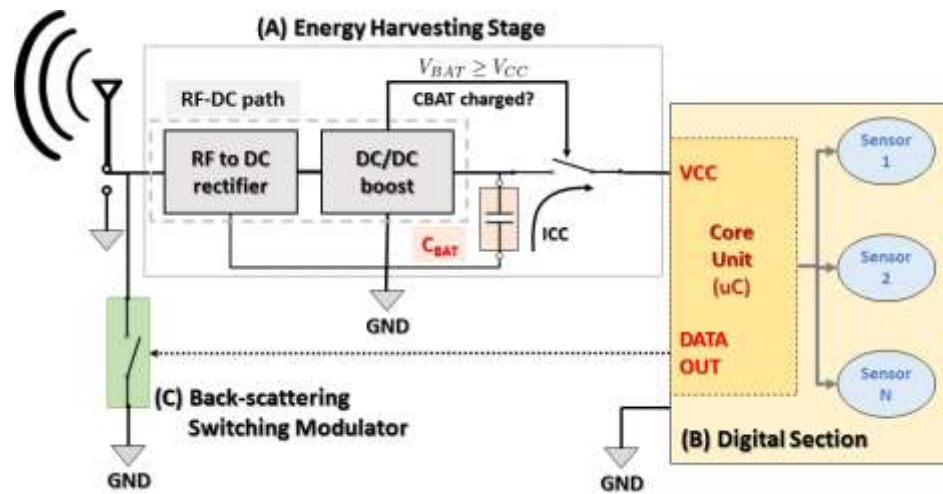
- The canceler for DSRC in real case can effectively reduce the interference



# Dedicated Short Range Vehicular Communications technologies

## Batteryless Transponder for Vehicular DSRC at 5.8 GHz

Conventional approach neglect the importance of the nonlinear effects in the rf-to-dc rectifier, with low dynamic termination



# Dedicated Short Range Vehicular Communications technologies

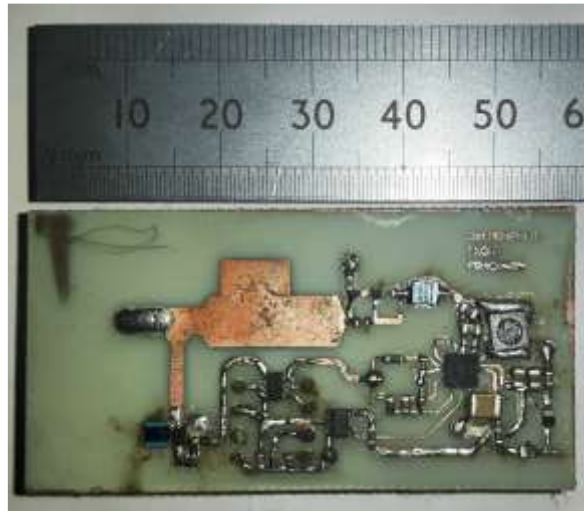
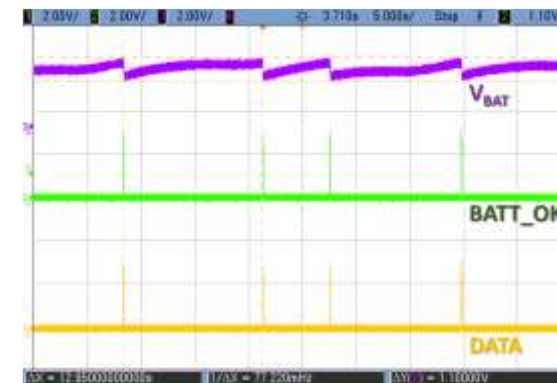


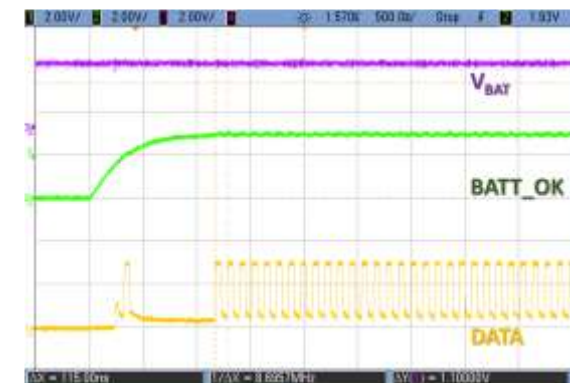
TABLE II: Harvesting performances at comparison with the state-of-the-art

Design	Harvesting Load and Conditions	Measured $P_{DC}$ ( $\mu\text{W}$ )	$\eta$	$I_{CHG}$ ; $\Delta T_{CHG}$
[43]	DC/DC, Current Sink 868 MHz, -5 dBm	-	-	-; 2.5 s
[4]	100 $\Omega$ , fixed load 2.4 GHz, -5 dBm	40.1	13%	118 $\mu\text{A}$ ; -
[2]	3000 $\Omega$ , fixed load 5.8 GHz, -5 dBm	72.7	23%	145 $\mu\text{A}$ ; -
[2]	DC/DC, Current Sink 5.8 GHz, 1 dBm	-	-	-; 140 s
This work	DC/DC, Current Sink 5.8 GHz, -5 dBm	51.0	16%	135 $\mu\text{A}$ ; 37 s
This work	DC/DC, Current Sink 5.8 GHz, -8 dBm	17.0	11%	50 $\mu\text{A}$ ; 100 s

Oscilloscope traces acquired with  $P_{RF} = -5 \text{ dBm}$   
Cyclic Packet Transmission



Transient of transmitted packet



## Car Talk



Alessandro Cidronali, Stefano Maddio,  
Marco Passafiume, and Gianfranco Manes

**T**he vision for intelligent transportation systems (ITS) in the near term foresees establishing radio communications between vehicles and the road infrastructure using the 5.9-GHz frequency band to propagate useful information aimed at passenger safety and efficient traffic management [1]-[3]. To date, three classes of applications have been distinguished at the communication application layer: road safety, traffic efficiency, and a catch-all category of other applications. All rely on roadside equipment (RSE) capable of broadcasting

other regulatory or contextual information along with onboard units (OBUs) capable of interacting with the RSE and, in some cases, of relaying the information to other vehicles.

In Europe, all these cases, along with others, are classified by the European Telecommunications Standards Institute (ETSI) [2]. Worldwide, over the years, other applications have been developed dedicated to answer specific needs of transport and safety. The most relevant are road tolls [4], [5] (see "Road Tolls: An An-

Alessandro Cidronali (alessandro.cidronali@iit.it), Stefano Maddio (stefano.maddio@iit.it), Marco Passafiume (marco.passafiume@iit.it) and Gianfranco Manes (gianfranco.manes@iit.it) are with the Department of Electronics Engineering, University of Florence, Italy.

Digital Object Identifier 10.1109/MMM.2016.2500499  
Date of publication: 22 October 2016





1. Passafiume, M., Collodi, G., & Cidronali, A. (2020). Design Principles of Batteryless Transponder for Vehicular DSRC at 5.8 GHz. *IEEE Journal of Radio Frequency Identification*.
2. Cidronali, A., Collodi, G., Lucarelli, M., Maddio, S., Passafiume, M., Pelosi, G., Assessment of anchors constellation features in rssi-based indoor positioning systems for smart environments, (2020) *Electronics (Switzerland)*, 9 (6), art. no. 1026, pp. 1-18.
3. Rojhani, N., Passafiume, M., Lucarelli, M., Collodi, G., Cidronali, A., Assessment of Compressive Sensing 2x2 MIMO Antenna Design for Millimeter-Wave Radar Image Enhancement, (2020) *Electronics (Switzerland)*, 9 (4), art. no. 624, .
4. Cidronali, A., Collodi, G., Pagnini, L., High-power UHF Doherty amplifier output combiner network optimization by 3-port sub-circuit X-parameters characterization.(2020) *Microwave and Optical Technology Letters*,
5. Cidronali, A., Collodi, G., Lucarelli, M., Maddio, S., Passafiume, M., Pelosi, G., Continuous Beam Steering for Phaseless Direction-of-Arrival Estimations, (2019) *IEEE Antennas and Wireless Propagation Letters*, 18 (12), art. no. 8873674, pp. 2666-2670.
6. Cidronali, A., Collodi, G., Large-signal vector characterization of LDMOS devices for analysis and design of broadband Doherty high-power amplifiers, (2019) *International Journal of Microwave and Wireless Technologies*, 11 (7), pp. 666-675.
7. Cidronali, A., Collodi, G., Maddio, S., Pelosi, G., Selleri, S., Quasi-elliptical band-pass filters based on compact spiral resonators for C-band applications, (2019) *Microwave and Optical Technology Letters*, 61 (8), pp. 1983-1987.
8. Cidronali, A., Collodi, G., Maddio, S., Passafiume, M., Pelosi, G., 2-D DoA Anchor Suitable for Indoor Positioning Systems Based on Space and Frequency Diversity for Legacy WLAN, (2018) *IEEE Microwave and Wireless Components Letters*, 28 (7), pp. 627-629.
9. Cidronali, A., Local Oscillator Phase-Dependent Linearized Mixer Modeling Based on Large-Signal Vector Measurements, (2018) *IEEE Transactions on Microwave Theory and Techniques*, 66 (1), art. no. 8038935, pp. 81-90.
10. Maddio, S., Cidronali, A., Passafiume, M., Collodi, G., Lucarelli, M., Maurri, S., Multipath Robust Azimuthal Direction of Arrival Estimation in Dual-Band 2.45-5.2 GHz Networks, (2017) *IEEE Transactions on Microwave Theory and Techniques*, 65 (11), art. no. 7929401, pp. 4438-4449
11. Passafiume, M., Maddio, S., Cidronali, A., An improved approach for RSSI-based only calibration-free real-time indoor localization on IEEE 802.11 and 802.15.4 wireless networks, (2017) *Sensors (Switzerland)*, 17 (4), art. no. 717,
12. Lucarelli, M., Maddio, S., Collodi, G., Cidronali, A., A wideband quadrature power splitter covering 81.75% fractional bandwidth in single layer via-less technology, (2017) *Microwave and Optical Technology Letters*, 59 (1), pp. 142-145.
13. Maddio, S., Cidronali, A., Passafiume, M., Collodi, G., Maurri, S., Fine-grained azimuthal direction of arrival estimation using received signal strengths, (2017) *Electronics Letters*, 53 (10), pp. 687-689.
14. Cidronali, A., Giovannelli, N., Maddio, S., Del Chiaro, A., Schuberth, C., Magesacher, T., Singerl, P., A 280 W LDMOS broadband Doherty PA with 52% of fractional bandwidth based on a multi-line impedance inverter for DVB-T applications, (2016) *International Journal of Microwave and Wireless Technologies*, 8 (8), pp. 1141-1153.
15. Maddio, S., Cidronali, A., Collodi, G., Base-band training of carrier leakage canceller in 5.8-GHz full-duplex transceivers, (2016) *Microwave and Optical Technology Letters*, 58 (11), pp. 2649-2653.
16. Cidronali, A., Maddio, S., Passafiume, M., Manes, G., Car Talk: Technologies for Vehicle-to-Roadside Communications, (2016) *IEEE Microwave Magazine*, 17 (11), art. no. 7590172, pp. 40-60.



17. Cidronali, A., Maddio, S., Giovannelli, N., Collodi, G., Frequency Analysis and Multiline Implementation of Compensated Impedance Inverter for Wideband Doherty High-Power Amplifier Design, (2016) IEEE Transactions on Microwave Theory and Techniques, 64 (5), art. no. 7460972, pp. 1359-1372.
18. Maddio, S., Passafiume, M., Cidronali, A., Manes, G., A Distributed Positioning System Based on a Predictive Fingerprinting Method Enabling Sub-Metric Precision in IEEE 802.11 Networks, (2015) IEEE Transactions on Microwave Theory and Techniques, 63 (12), art. no. 7331340, pp. 4567-4580.
19. Maddio, S., Cidronali, A., Manes, G., Real-time adaptive transmitter leakage cancelling in 5.8-GHz full-duplex transceivers, (2015) IEEE Transactions on Microwave Theory and Techniques, 63 (2), art. no. 7014308, pp. 509-519.
20. Cidronali, A., Maddio, S., Collodi, G., Manes, G., Design trade-off for a compact 5.8 GHz DSRC transponder front-end, (2015) Microwave and Optical Technology Letters, 57 (5), pp. 1187-1191.
21. Cidronali, A., Giovannelli, N., Mercanti, M., Maddio, S., Manes, G., Concurrent dual-band envelope tracking GaN PA design and its 2D shaping function characterization, (2013) International Journal of Microwave and Wireless Technologies, 5 (6), pp. 669-681.
22. Cidronali, A., Mercanti, M., Giovannelli, N., Maddio, S., Manes, G., On the signal probability distribution conscious characterization of GaN devices for optimum envelope tracking PA design, (2013) IEEE Microwave and Wireless Components Letters, 23 (7), art. no. 6518199, pp. 380-382.
23. Fagotti, R., Cidronali, A., Manes, G., Concurrent hex-band GaN power amplifier for wireless communication systems, (2011) IEEE Microwave and Wireless Components Letters, 21 (2), art. no. 5711406, pp. 89-91.
24. Maddio, S., Cidronali, A., Manes, G., A new design method for single-feed circular polarization microstrip antenna with an arbitrary impedance matching condition, (2011) IEEE Transactions on Antennas and Propagation, 59 (2), art. no. 5648755, pp. 379-389.
25. Cidronali, A., Maddio, S., Giorgetti, G., Manes, G., Analysis and performance of a smart antenna for 2.45-GHz single-anchor indoor positioning, (2010) IEEE Transactions on Microwave Theory and Techniques, 58 (1), art. no. 5338029, pp. 21-31.
26. Magrini, I., Cidronali, A., Manes, G., A low local oscillator power k-band mixer based on tunneling diodes, (2009) Microwave and Optical Technology Letters, 51 (4), pp. 1140-1143.
27. Cidronali, A., Magrini, I., Giovannelli, N., Mercanti, M., Manes, G., Experimental system level analysis of a concurrent dual-band power amplifier for WiMAX and WCDMA applications, (2009) International Journal of Microwave and Wireless Technologies, 1 (2), pp. 99-107.
28. Camarchia, V., Giofrè, R., Magrini, I., Piazzon, L., Cidronali, A., Colantonio, P., Guerrieri, S.D., Ghione, G., Giannini, F., Pirola, M., Manes, G., Concurrent dual-band SiGe HBT power amplifier for Wireless applications, (2009) International Journal of Microwave and Wireless Technologies, 1 (2), pp. 117-126.
29. Giorgetti, G., Cidronali, A., Gupta, S.K.S., Manes, G., Single-anchor indoor localization using a switched-beam antenna, (2009) IEEE Communications Letters, 13 (1), pp. 58-60.
30. Cidronali, A., Magrini, I., Fagotti, R., Alimenti, F., Mercanti, M., Manes, G., Dynamic biasing in SiGe HBT for wideband step envelope tracking power amplifiers, (2008) International Journal of RF and Microwave Computer-Aided Engineering, 18 (6), pp. 564-573.
31. Colantonio, P., Giannini, F., Giofrè, R., Piazzon, L., Camarchia, V., Pirola, M., Ghione, G., Cidronali, A., Magrini, I., Manes, G., Scholz, R., Knoll, D., From device characterization to system level analysis of dual band PA design in SiGe technology, (2008) International Journal of RF and Microwave Computer-Aided Engineering, 18 (6), pp. 552-563



32. Cidronali, A., Accillaro, C., Manes, G. Mildly nonquasi-static two-port device model extraction by integrating linearized large-signal vector measurements, (2007) IEEE Transactions on Microwave Theory and Techniques, 55 (11), pp. 2277-2288.
33. Cidronali, A., Loglio, G., Manes, G., Linearized frequency conversion properties of two-port devices as a function of the pumping signal amplitude and phase, (2006) International Journal of RF and Microwave Computer-Aided Engineering, 16 (6), pp. 612-624.
34. Cidronali, A., Loglio, G., Jargon, J., Manes, G., Behavioral model for reducing the complexity of mixer analysis and design, (2005) International Journal of RF and Microwave Computer-Aided Engineering, 15 (4), pp. 362-370.
35. Jargon, J., Gupta, K.C., Cidronali, A., DeGroot, D., Expanding definitions of gain by taking harmonic content into account, (2003) International Journal of RF and Microwave Computer-Aided Engineering, 13 (5), pp. 357-369.
36. Cidronali, A., Nair, V., Collodi, G., Lewis, J.H., Camprini, M., Manes, G., Goronkin, H., MMIC applications of heterostructure interband tunnel devices, (2003) IEEE Transactions on Microwave Theory and Techniques, 51 (4 II), pp. 1351-1367.
37. Cidronali, A., Leuzzi, G., Manes, G., Giannini, F., Physical/electromagnetic pHEMT modeling, (2003) IEEE Transactions on Microwave Theory and Techniques, 51 (3), pp. 830-838.
38. Cidronali, A., Collodi, G., Santarelli, A., Vannini, G., Manes, G., Millimeter-wave FET modeling using on-wafer measurements and EM simulation, (2002) IEEE Transactions on Microwave Theory and Techniques, 50 (2), pp. 425-432.
39. Cidronali, A., Collodi, G., Camprini, M., Nair, V., Manes, G., Lewis, J., Goronkin, H., Ultralow DC power VCO based on InP-HEMT and heterojunction interband tunnel diode for wireless applications, (2002) IEEE Transactions on Microwave Theory and Techniques, 50 (12), pp. 2938-2946.
40. Cidronali, A., Collodi, G., Camprini, M., Nair, V., Manes, G., Lewis, J., Goronkin, H., Ultra low-power VCO based on InP-HEMT and heterojunction interband tunnel diode for wireless application, (2002) IEEE MTT-S International Microwave Symposium Digest, 1, pp. 43-46.
41. Cidronali, A., Collodi, G., Deshpande, M.R., El-Zein, N., Nair, V., Manes, G., Goronkin, H., A highly linear single balanced mixer based on heterojunction interband tunneling diode, (2001) IEEE Transactions on Microwave Theory and Techniques, 49 (12), pp. 2437-2445.
42. Cidronali, A., Collodi, G., Deshpande, M., Toccafondi, C., El-Zein, N., Manes, G., Nair, V., Goronkin, H., Modeling and investigation of instabilities in Heterojunction Interband Tunnel Diodes for microwave applications(2001) IEEE MTT-S International Microwave Symposium Digest, 2, pp. 1269-1272.
43. Cidronali, A., Collodi, G., Vannini, G., Santarelli, A., Manes, G., Anew approach to FET model scaling and MMIC design based on electromagnetic analysis, (1999) IEEE Transactions on Microwave Theory and Techniques, 47 (6 PART 2), pp. 900-907.
44. Cidronali, A., Collodi, G., Vannini, G., Santarelli, A., Small-signal distributed FET model consistent with device scaling, (1999) Electronics Letters, 35 (5), pp. 371-372.
45. Ayitabile, G., Cidronali, A., Manes, G., S-band digital downconverter for radar applications based on a GaAs MMIC fast sample-and-hold, (1996) IEE Proceedings: Circuits, Devices and Systems, 143 (6), pp. 337-342.